The University of Reading

Simple Models of Changing Bathymetry with Data Assimilation

P.J. Smith[1], M.J. Baines[1], S.L. Dance[1], N.K. Nichols[1] and T.R. Scott[2]

NUMERICAL ANALYSIS REPORT 10/2007

[1] *Department of Mathematics*
The University of Reading
Whiteknights, PO Box 220
Reading, RG6 6AX

[2] *Environmental Systems Science Centre*
The University of Reading
Early Gate,
Reading, RG6 6AL

Department of Mathematics

Simple Models of Changing Bathymetry with Data Assimilation

P.J. Smith, M.J. Baines, S.L. Dance, N.K. Nichols, T.R. Scott

November 2007

Abstract

Data assimilation is a means for combining observational data with model predictions to produce a model state that most accurately estimates the current and future states of the true system. The technique is commonly used in atmospheric and oceanic modelling, but in this report we consider its application within a coastal environment. A simplified one-dimensional model of bedform propagation is used to illustrate the basic theory of data assimilation and examine some of the issues associated with its practical implementation. The equations used to describe the morphodynamic evolution of the seabed are introduced and the method of characteristics is used to derive a solution in the special case of constant water height and flux. We then present a general overview of the principles of data assimilation and describe the optimal interpolation scheme used in this work. The roles of the background and observation error covariance matrices are discussed. Particular attention is given to the background error correlations and the way in which they govern the spatial spreading and smoothing of information from the observations. A simple model based on the linear advection equation is used to set up a series of test cases to investigate the effect of alternative forms for the background error covariance matrix, with results validated against the analytical solution. It is shown that when the background error correlations are poorly specified the quality of the analysis is greatly reduced.

1 Introduction

Changes to UK weather patterns, with increasing incidence of coastal flooding in recent years, have led to growing concern over the effects of climate change [Lowe and Gregory (2005)]. It is essential that we improve our ability to predict floods; being able to better identify and anticipate flood risk would facilitate the development of suitable strategies for the management of coastal areas and help to limit the damage and distress caused by flooding. Key to this is better knowledge and understanding of how the morphology of the coastal zone is evolving over time [Nicholls et al. (2007), Stelling (2000)].

Bathymetry is the underwater equivalent to topography used to describe the elevation of the sea floor. The bathymetry of the coastline changes as sediment is eroded, transported and deposited by water action. The change in bathymetry alters the water flow, which further changes the bathymetry, which in turn alters the motion of the water, and so on. Coastal morphodynamics is the study of the evolution of the bathymetry in response to the flow induced sediment transport [Soulsby (1997)]. It is a particularly challenging area; an effective coastal morphodynamic model must be able to represent the continual interaction between water flow and bathymetry in the coastal zone. Modelling is difficult because longer term morphological changes are driven by shorter term processes such as waves, tides and river outflows [Masselink and Hughes (2003)]. In practice, models suffer from uncertainty in their initial conditions and parameters which can lead to significant errors

between the predicted and actual states of the system, so that coastal morphodynamic models often perform poorly in detail [Nicholson et al. (1997), Sutherland et al. (2004)]. Improved accuracy of such models would allow better prediction of future bathymetry, enabling improved flood forecasting and providing an important tool for coastal management. State of the art coastal morphodynamic models are growing more and more sophisticated in an attempt to do this [e.g. Lesser et al. (2004)]. A complementary approach to improving model performance is to combine model integrations with observations of bathymetry using data assimilation techniques.

Data assimilation is a technique for combining observational data with model predictions to produce a model state that most accurately estimates the current and future states of the true system. It is routinely used in atmospheric and oceanic prediction, but the possibility of transferring the method to the coastal environment has only recently been investigated [Scott and Mason (2007)].

Observations of bathymetry are available from a variety of sources, including remotely sensed waterlines, swath bathymetry, beach transects, X-band radar and LiDAR data [Mason et al. (2000)]. These observations may be infrequent and samples typically only provide partial coverage of the model domain, but data assimilation, together with the dynamics of the model, enables us to use these limited data efficiently and effectively.

In reality, a model cannot represent the behaviour of a morphodynamic system exactly. Over time the model bathymetry will diverge from the true bathymetry and errors will arise due to imperfect initial conditions and inaccuracies in physical parameters and numerical implementation. Data assimilation can be used to compensate for the inadequacies of a model and help keep the model bathymetry on track. By periodically incorporating measured observations into the model, data assimilation nudges the model bathymetry back toward the true bathymetry, thus improving the ability of the model to predict future bathymetry.

The aim of this report is to use a simplified one-dimensional model of changing bathymetry to understand the basic theory of data assimilation. By exploring how a simple system behaves under varied conditions we gain insight into some of the theoretical issues that need to be considered when applying data assimilation to a full coastal morphodynamic model.

In section 2 we introduce the equations used to describe the morphodynamic evolution of the seabed in one-dimension, and use the method of characteristics to derive a solution for the special case of constant water height and flux. In section 3 we give a brief mathematical overview of data assimilation and describe the sequential method used in this work. In section 4.1 we build a simple model based on the ideas presented in section 2, but simplified to avoid the complexities associated with a non-linear bed celerity. This simple model is a linear advection equation. In section 4.2 we explain how the model will be implemented and outline the steps of the assimilation algorithm. In section 4.4 we discuss the roles of the background and observation error covariance matrices. We pay particular attention to the background error correlations and the way in which they govern the spatial spreading and smoothing of information from the observations. In section 4.5 we consider three alternative forms for the background error covariance matrix and set up a series of experiments to examine the effect of each matrix for different combinations of observations. Section 5 presents the results of these experiments, comparing them with the analytical solution to the linear advection equation. Finally, in section 6 we outline the conclusions that can be drawn from this work and propose areas for development and further study.

2 The sediment conservation equation

Changes in bathymetry due to flow induced sediment transport processes can be described using the sediment conservation equation [Soulsby (1997)]. In this report we consider a simple one dimensional version,

$$\frac{\partial z}{\partial t} = -\left(\frac{1}{1-\varepsilon}\right)\frac{\partial q}{\partial x}, \tag{2.1}$$

in the x direction, where $z(x,t)$ is the bathymetry, t is the time, q is the total (suspended and bedload) sediment transport rate, and ε is the sediment porosity. If $\frac{\partial z}{\partial t}$ is positive accretion is occurring, and if $\frac{\partial z}{\partial t}$ is negative erosion is occurring.

2.1 Calculating the sediment transport rate

Before we can solve (2.1), the sediment transport rate q needs to be estimated; this can be done using the power law equation

$$q = Au^n, \tag{2.2}$$

where $u = u(x,t)$ is the depth averaged current and A and n are parameters whose values need to be set.

This is a simplified version of a formula derived by van Rijn (1993) to parameterise the results of his sediment transport theory and is based on a mixture of fundamental physics and empirical results. A variety of alternative formulae have been proposed, many of which are presented in Soulsby (1997).

2.2 Solving the 1D sediment conservation equation

To solve (2.1) we rewrite it in the quasi linear form

$$\frac{\partial z}{\partial t} + a(z,q)\frac{\partial z}{\partial x} = 0, \tag{2.3}$$

where

$$a(z,q) = \left(\frac{1}{1-\varepsilon}\right)\frac{\partial q}{\partial z}. \tag{2.4}$$

The coefficient $a(z,q)$ is often referred to as the advection velocity or bed celerity. It is a non-linear function, depending on the bathymetry z both directly and through the sediment transport rate q.

By assuming that the water height and flux are constant, and setting $u(h-z) = F$, where h is water height and F is water flux, we can rewrite q in a form that can be differentiated with respect to z

$$q = A\left(\frac{F}{h-z}\right)^n. \tag{2.5}$$

Hence, we obtain the following expression for $a(z,q) = a(z)$

$$a(z) = \frac{nAF^n}{1-\varepsilon}\left(h-z\right)^{-(n+1)}. \tag{2.6}$$

The sediment conservation equation (2.3) can now be solved using the method of characteristics [LeVeque (1992)].

2.3 Characteristics

Consider the chain rule for taking the total derivative of z with respect to t,

$$\frac{dz}{dt} = \frac{\partial z}{\partial t} + \frac{dx}{dt}\frac{\partial z}{\partial x}.$$

Using equation (2.3) to substitute for $\frac{\partial z}{\partial t}$ we obtain

$$\frac{dz}{dt} = \left(\frac{dx}{dt} - a(z)\right)\frac{\partial z}{\partial x}.$$

Note that

$$\frac{dz}{dt} = 0 \text{ along the curves given by } \frac{dx}{dt} = a(z). \tag{2.7}$$

These curves are called the *characteristics* of the equation, and from (2.7) we can see that $z(x,t)$ takes a constant value on each. We can use this property to construct a solution to (2.3).

Since $z(x,t)$ is constant on any given characteristic so too is the slope of the characteristic $a(z)$, thus the characteristics are straight lines given by

$$x = x_0 + a(z_0)t. \tag{2.8}$$

Here, $z_0 = z(x_0, 0)$ is the value of z on the characteristic, determined by the initial data and x_0 is the point of intercept of the characteristic with the x axis (figure 2.1).

To obtain a value for the solution $z(x,t)$ at a point x at time t we trace back along the characteristic (2.8) to the initial data. The solution is given implicitly by

$$z(x,t) = z(x_0,0) = z(x - a(z(x,t))t, 0) \qquad \text{for } t \geq 0. \tag{2.9}$$

This concept is illustrated in figure 2.1 for an initial bathymetry given by the Gaussian exponential function

$$z(x,0) = \alpha e^{-\beta(x-\gamma)^2}, \tag{2.10}$$

where α, β and γ are constants whose values determine the height, width and position of the curve respectively.

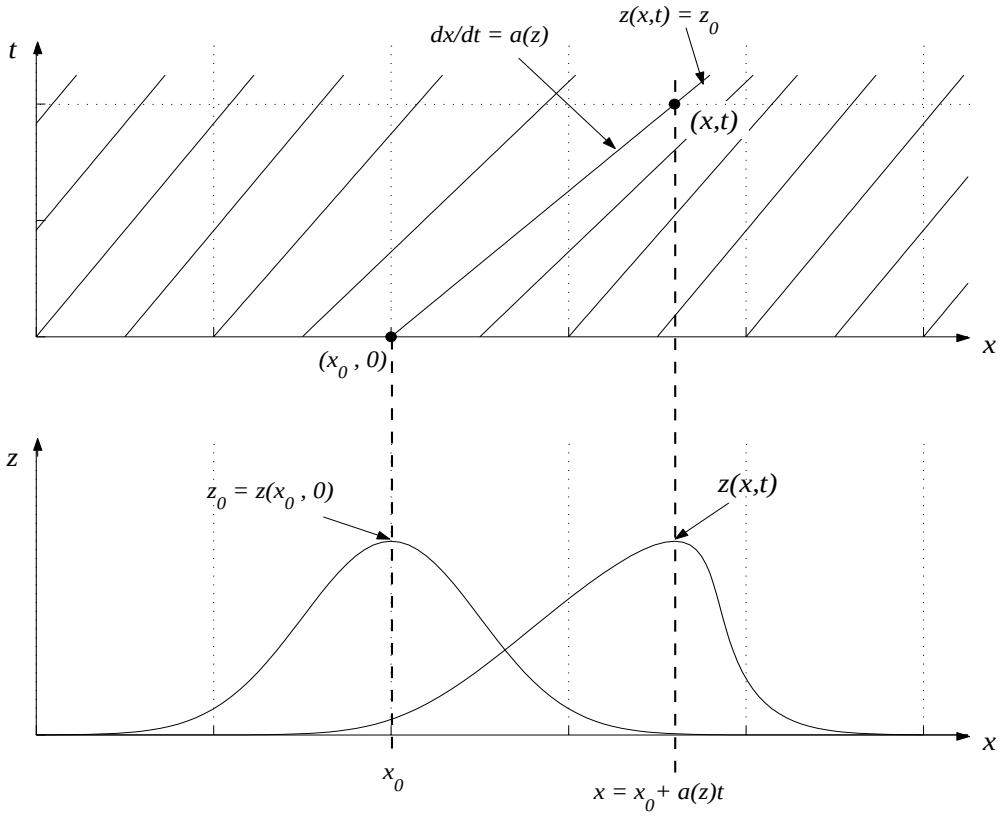

Figure 2.1: Characteristics and solutions to the sediment conservation equation for Gaussian initial data.

3 Data Assimilation

The aim of data assimilation is to combine measured observations of a system with model predictions to derive a model state that most accurately describes the true state of the system. This optimal estimate is called the *analysis*.

A wide variety of data assimilation schemes exist, many of which have been derived using statistical techniques [e.g. Griffith (1997), Kalnay (2003)]. In section 3.1 we present two standard methods based on statistical estimation theory: *optimal interpolation* (OI) and *three dimensional variational data assimilation* (3D Var).

3.1 Optimal interpolation and 3D variational data assimilation

The OI method belongs to a group of schemes described as *sequential*. It is a widely used technique originally designed for a system in which the observations are linearly related to the model state variables. Sequential data assimilation algorithms step through the observations in order using them at the time they become available.

3D Var schemes are designed to provide an analysis at a single time. They do not take account of the time dependency of observations, but treat all observations as if they had been made at the same time. If a 3D Var scheme is applied cyclically it can be regarded as a sequential method.

OI seeks to minimize the analysis error variance by finding an analysis state that is as close as possible to the true state in a root mean square (r.m.s) sense. 3D Var data assimilation can be viewed as a different approach to solving the same problem as OI. It is based on a maximum a posteriori estimate approach and derives the analysis by looking for a state that minimizes a cost function measuring its distance from the background and observations.

If we assume random, unbiased, Gaussian errors the minimum variance and maximum a posteriori estimates coincide. We can therefore find the analysis by minimising a least squares cost function [Lewis et al. (2006)].

3.2 The cost function

We suppose that the true state of the system is represented by a vector $\mathbf{z^t} \in \mathbb{R}^m$, and that we have a *background* estimate $\mathbf{z^b} \in \mathbb{R}^m$, based on some prior knowledge of what we expect the present state to be. We suppose also that we have a vector $\mathbf{y} \in \mathbb{R}^p$ containing p observations to be assimilated and an observation operator $\mathbf{h} : \mathbb{R}^m \longrightarrow \mathbb{R}^p$ that maps from model to observation space. If we have direct observations, $\mathbf{h}$ is simply an interpolation operator for interpolating variables from the model grid to observation locations. Often, the model variables we wish to analyse cannot be observed directly and instead we have observations of another measurable quantity. In this case, $\mathbf{h}$ will also include transformations based on physical relationships that convert the model variables to the observations. For example, when assimilating observations of water depth into a morphodynamic model, the observation operator interpolates the predicted model bathymetry to the observation locations and then converts it into predicted values for the water depth [Scott and Mason (2007)].

We wish to optimally combine the background $\mathbf{z^b}$ and observations $\mathbf{y}$ to produce an analysis state $\mathbf{z^a} \in \mathbb{R}^m$ that gives the best possible estimate of the true system state $\mathbf{z^t}$.

We define a cost function $J(\mathbf{z})$ that measures the distance of the solution from the background and observations weighted by the inverse of their errors

$$J(\mathbf{z}) = (\mathbf{z} - \mathbf{z^b})^{\mathbf{T}}\mathbf{B^{-1}}(\mathbf{z} - \mathbf{z^b}) + (\mathbf{y} - \mathbf{h}(\mathbf{z}))^{\mathbf{T}}\mathbf{R^{-1}}(\mathbf{y} - \mathbf{h}(\mathbf{z})), \tag{3.1}$$

where $\mathbf{z} \in \mathbb{R}^n$ is the model state vector, and $\mathbf{B} \in \mathbb{R}^{m \times m}$ and $\mathbf{R} \in \mathbb{R}^{p \times p}$ are the covariance matrices of the background and observation errors.

To determine the particular $\mathbf{z}$ that minimises $J(\mathbf{z})$ we differentiate (3.1) with respect to $\mathbf{z}$ and derive an expression for the gradient vector $\nabla J(\mathbf{z})$. The analysis ($\mathbf{z^a}$) is then given by the solution of

$$\nabla J(\mathbf{z^a}) = \mathbf{2B^{-1}}(\mathbf{z^a} - \mathbf{z^b}) - \mathbf{2H^T R^{-1}}(\mathbf{y} - \mathbf{h}(\mathbf{z^a})) = \mathbf{0}, \tag{3.2}$$

where $\mathbf{H} \in \mathbb{R}^{p \times m}$ is the linearisation (Jacobian) of $\mathbf{h}$.

Using the tangent linear hypothesis [Bouttier and Courtier (2002)] we have

$$\mathbf{h}(\mathbf{z^a}) - \mathbf{h}(\mathbf{z^b}) \approx \mathbf{H}(\mathbf{z^a} - \mathbf{z^b}).$$

Inserting this into (3.2) and rearranging gives

$$\mathbf{z^a} = \mathbf{z^b} + \mathbf{K}[\mathbf{y} - \mathbf{h}(\mathbf{z^b})]. \tag{3.3}$$

The operator $\mathbf{K} \in \mathbb{R}^{m \times p}$ is called the gain matrix [Nichols (2003)] and determines the weight given to the observations. It is given by

$$\mathbf{K} = \mathbf{B}\mathbf{H}^{\mathbf{T}}(\mathbf{H}\mathbf{B}\mathbf{H}^{\mathbf{T}} + \mathbf{R})^{-\mathbf{1}}. \tag{3.4}$$

By choosing $\mathbf{K}$ correctly, we can ensure that the analysis states will converge to the true states of the system over time [Jazwinski (1970)].

This is the formal solution to the optimization problem. The OI method uses (3.4) to calculate the matrix $\mathbf{K}$ explicitly and solve (3.3) directly. The idea of 3D Var is to avoid computation of the gain matrix $\mathbf{K}$ and in practice the analysis is obtained iteratively through use of a suitable descent/ minimization algorithm [Bouttier and Courtier (2002), Lewis et al. (2006)].

When the observation operator $\mathbf{h}$ is linear the 3D Var and OI solutions are equivalent and we can use OI to understand how variational assimilation works [Lewis et al. (2006)]. Since the dimensions of our model are small $\mathbf{K}$ is relatively easy to compute. We will therefore adopt the OI method in this work. On an operational scale OI becomes impractical and it is more efficient to apply a 3D Var approach.

4 The model

The primary purpose of this report is to investigate and understand some of the basic principles of data assimilation. For simplicity, we wish to choose a model that we can solve analytically, but with $a(z)$ of the form (2.6) equation (2.3) is non-linear and equation (2.8) for x_0 is implicit. The model used for this work will therefore be based on the ideas presented in section 2, but with the bed celerity $a(z)$ replaced with a, where a is a constant to be chosen.

4.1 The linear advection equation

We assume that the advection velocity is constant, replacing $a(z)$ with a constant a. Equation (2.3) then reduces to

$$\frac{\partial z}{\partial t} + a\frac{\partial z}{\partial x} = 0. \tag{4.1}$$

This equation is known as the linear advection equation. It differs from the sediment conservation equation (2.3) in that it assumes the advection velocity a is independent of z and q. Its characteristic equations (2.8) are not implicit and this makes it much easier to solve. Its solution is simply

$$z(x,t) = z(x_0,0) = z(x-at,0) \qquad \text{for } t \geq 0. \tag{4.2}$$

Figures 4.1 and 4.2 illustrate the effect of setting $a(z)$ to be constant. The solution (2.9) for the sediment conservation equation, with initial bathymetry given by (2.10), represents a smooth, bell-shaped bedform that propagates downstream with velocity $a(z)$. Since $a(z)$ is non-constant the initial profile becomes distorted, gradually steepening until it begins to overturn. In the simple

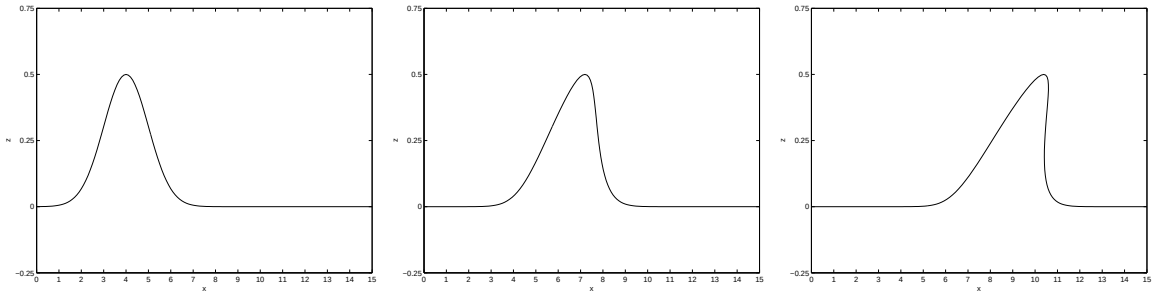

Figure 4.1: Solution to the sediment conservation equation with constant water height and flux.

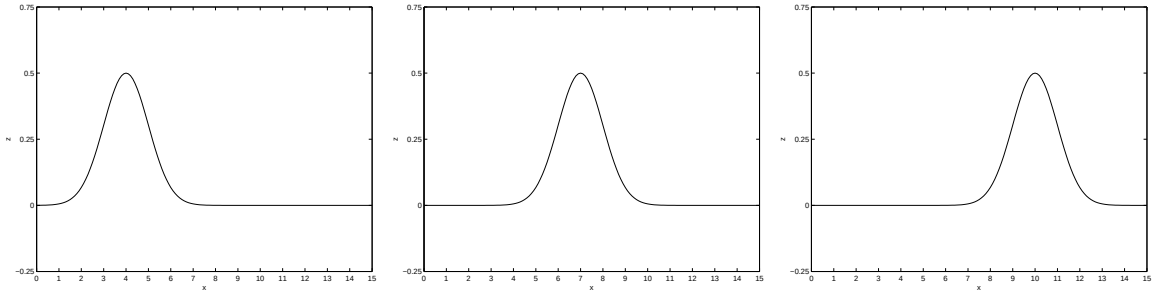

Figure 4.2: Solution to the linear advection equation.

advection case, the solution (4.2) represents a direct translation of the initial data. The bed now moves undistorted across the domain with constant speed a.

Using the linear advection equation (4.1) as opposed to equation (2.3) allows us to solve the assimilation problem analytically and provides a simple reference solution against which we can evaluate the performance of our model.

4.2 Model setup

We assume that the morphodynamic evolution of the true system is described by the advection equation (4.1) with initial bathymetry given by (2.10). Starting from a perturbed initial state and using observations taken from the true solution we wish to examine the effectiveness of data assimilation in helping to nudge the bathymetry back toward the true state as we move forward in time. The analytical solution (4.2) with exact initial data (2.10) will be used as a reference against which to assess the performance of the model.

4.3 The assimilation algorithm

The assimilation cycle can be split into two main phases [Kalnay (2003)]:

1. The *forecast* phase in which the analysis from the previous time step $\mathbf{z^a}(t_k)$ is integrated forward using the forecast model (in this case the 'model' is the translation given by the advection velocity a) to become the background state $\mathbf{z^b}$ at analysis time t_{k+1}. At the start of the first forecast phase an *a priori* estimate for the initial background state $\mathbf{z^b}(t_0) = \mathbf{z_0^b}$ needs to be chosen.

2. The *analysis* phase in which the difference between the predicted observations given by the new background state $\mathbf{z^b}(t_{k+1})$ and the vector of measured observations $\mathbf{y}(t_{k+1})$ is used in equation (3.3) to produce an updated analysis state $\mathbf{z^a}(t_{k+1})$. Observations are taken at the start of each analysis phase; they are used only once, at the correct time, and not again.

Once the analysis phase is complete we advance to the start of the next cycle and the process is repeated.

4.4 The error covariance matrices

Before we can implement our assimilation algorithm we need to make estimates of the background and observation error covariance matrices $\mathbf{B}$ and $\mathbf{R}$. We are assuming that our model is perfect, but in practice the model equations do not describe the system behaviour completely, the background state is not known exactly and the measured observations are imprecise. Our assimilation scheme needs to take account of the errors that arise as a result of these inaccuracies as the precision of the analysis is determined by the precision of the background and observations. The error covariance matrices $\mathbf{B}$ and $\mathbf{R}$ represent our uncertainty in the background $\mathbf{z^b}$ and observations $\mathbf{y}$ and their specification has an important effect on the quality of the analysis.

The observation error covariance matrix $\mathbf{R}$ gives a statistical description of the errors in $\mathbf{y}$. Observation errors originate from instrumental error, errors in the forward model $\mathbf{h}$ and representativeness errors [Bouttier and Courtier (2002)]. Generally, it is reasonable to assume that errors in measurements taken at different locations are uncorrelated, in which case the matrix $\mathbf{R}$ is diagonal.

The background error covariance matrix $\mathbf{B} = \{b_{ij}\}$ describes the estimation errors of the background state, where element b_{ij} defines the error covariance between components i and j of $\mathbf{z^b}$. It is the last operator to act in (3.4) and is therefore fundamental in determining the nature of the analysis increment. The correlations in $\mathbf{B}$ govern the smoothing and spreading of information from the observations, determining how an observation at one point influences the analysis at nearby points [Bouttier and Courtier (2002)]. In noisy, observation dense regions, the background error correlations are used to ensure that the analysis is smooth and contains scales that are statistically compatible with the smoothness properties of the physical fields. In data sparse regions, where there are few observations, correlations are needed to spread the information contained in the available observations to the surrounding domain. Correct specification of the matrix $\mathbf{B}$ offers a significant challenge, and has a vital impact on the assimilation results.

4.5 The experiments

To initiate the assimilation cycle we require a first guess for the background state. For these experiments $\mathbf{z_0^b}$ was taken to be of the same form as the initial bathymetry for the truth (2.10) but with slightly modified values for α, β and γ.

The observations are to be taken from the true solution and for ease of computation we want the the observation points to coincide with the model grid so that the observation operator $\mathbf{h}$ is linear and $\mathbf{h} = \mathbf{H}$. We set

$$y_j = z_j^t,$$

where y_j is the observation of the true bathymetry z_j^t, given by (4.2), at the grid point x_j. The set of grid points x_j at which observations are to be taken is determined at the start of the assimilation process and remains fixed throughout. As our algorithm is sequential, a new set of observations is used during each cycle. Since the observations are taken from the truth, we weight in their favour, setting the observation and background variances to be $\sigma_o^2 = 0.1$ and $\sigma_b^2 = 1$ respectively.

We assume that the observation errors are uncorrelated and take the observation error covariance matrix $\mathbf{R}$ to be diagonal with variance σ_o^2. We consider three different ways of computing the background error covariance matrix $\mathbf{B}$:

To begin, we assume that the matrix $\mathbf{B}$ is diagonal with variance σ_b^2, i.e.

$$\mathbf{B} = \sigma_b^2 \mathbf{I}, \qquad \mathbf{I} \in \mathbb{R}^{m \times m}. \tag{4.3}$$

However, this is a poor approximation as it ignores correlations between grid points and means that observations have no effect on their neighbouring points.

Next, we add entries above and below the main diagonal by setting

$$b_{i-1,i} = b_{i,i-1} = \frac{\sigma_b^2}{2}, \qquad i = 2, \ldots, m.$$

This gives a tri-diagonal matrix $\mathbf{B}$ of the form

$$\mathbf{B} = \begin{pmatrix} \sigma_b^2 & \frac{\sigma_b^2}{2} & 0 & \cdots & \cdots & \cdots & 0 \\ \frac{\sigma_b^2}{2} & \sigma_b^2 & \frac{\sigma_b^2}{2} & 0 & & & \vdots \\ 0 & \ddots & \ddots & \ddots & \ddots & & \vdots \\ \vdots & \ddots & \ddots & \ddots & \ddots & \ddots & \vdots \\ \vdots & & \ddots & \ddots & \ddots & \ddots & 0 \\ \vdots & & & \ddots & \frac{\sigma_b^2}{2} & \sigma_b^2 & \frac{\sigma_b^2}{2} \\ 0 & \cdots & \cdots & \cdots & 0 & \frac{\sigma_b^2}{2} & \sigma_b^2 \end{pmatrix}. \tag{4.4}$$

Finally, we use the gaussian exponential function [Daley (1991), Kalnay (2003)]

$$b_{ij} = \sigma_b^2 e^{-r_{ij}^2/2L^2}, \tag{4.5}$$

to construct a matrix $\mathbf{B}$ with full off diagonal entries. Here $r_{ij}^2 = (x_i - x_j)^2$ is the square of the distance between the grid points x_i and x_j, and L is the background correlation length scale. The form (4.5) assumes that the covariance between the background errors at two grid points depends only on the spatial distance between them and that covariances decrease with separation distance. The background correlation length scale L can be used to determine the domain of influence of observations.

The assimilation was run for each of the different $\mathbf{B}$ matrices, experimenting with various combinations of observations, and validating the results against the analytic solution. The effect of L in (4.5) was also investigated, using the analysis errors $\varepsilon_{\mathbf{a}} = \mathbf{z_a} - \mathbf{z_t}$ to try to determine its optimal value for different observation strategies. Results are presented in the following section.

5 Results

5.1 The Matrix B

Figures 5.1 to 5.3 compare the analysis produced at initial time t_0 for each of the background covariance matrices discussed in section 4.4. Results are shown for six different observation schemes on the domain $x \in [0, 10]$ with grid spacing $\Delta x = 0.25$. The dot-dash line represents the true bathymetry $\mathbf{z^t}$. Observations $\mathbf{y}$ are given by circles, the background $\mathbf{z^b}$ by the dashed line and the analysis $\mathbf{z^a}$ by the solid line.

When both $\mathbf{B}$ and $\mathbf{R}$ are diagonal the expression for the gain matrix $\mathbf{K}$ simplifies and the analysis equation (3.3) reduces to

$$\mathbf{z^a} = \mathbf{z^b} + \frac{\sigma_\mathbf{b}^\mathbf{2}}{\sigma_\mathbf{o}^\mathbf{2} + \sigma_\mathbf{b}^\mathbf{2}}[\mathbf{y} - \mathbf{h}(\mathbf{z^b})].$$

$\mathbf{K}$ now acts like a scalar, this means that each observation only effects the value of the analysis at the grid point at which it is taken. At points where there are observations the analysis is given by a weighted average of z_j^b and y_j. Since we have taken $\sigma_o^2 \gg \sigma_b^2$, a relatively small weight is given to the background state and the analysis lies close to the observed value. At grid points where no observation is taken the analysis is set to the background, resulting in a jagged analysis curve (figure 5.1).

Similar results are produced with the tri-diagonal matrix $\mathbf{B}$ (figure 5.2), except that the observational information is now spread to neighbouring grid points and so also affects the analysis at points either side of the observation. Unless observations are taken at at least every other grid point, this still leaves regions where the available observations have no effect on the analysis and therefore generates oscillations as above.

The gaussian matrix $\mathbf{B}$ produces a much smoother analysis (figure 5.3). $\mathbf{B}$ now has a much larger radius of influence and the information contained in the observations is spread further into the domain. Each observation now affects more of the surrounding grid points allowing the shape of the true bathymetry to be more accurately captured with fewer observations.

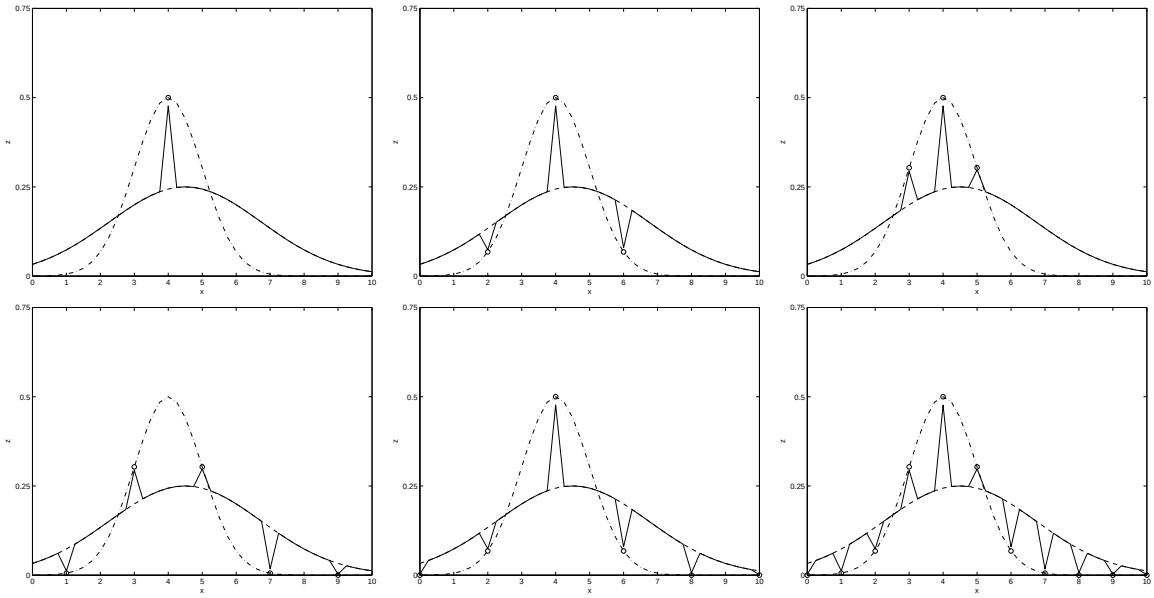

Figure 5.1: Diagonal matrix $\mathbf{B}$ - initial analysis for different observation combinations. The dot-dash line represents the true bathymetry $\mathbf{z^t}$. Observations $\mathbf{y}$ are given by circles, the background $\mathbf{z^b}$ by the dashed line and the analysis $\mathbf{z^a}$ by the solid line.

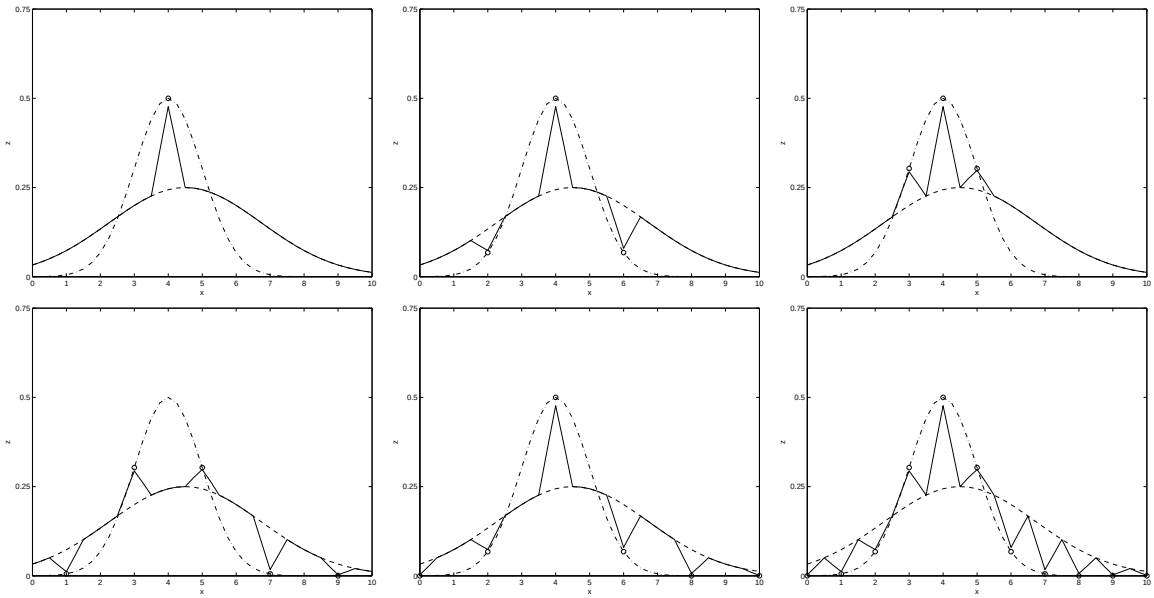

Figure 5.2: Tri-diagonal matrix $\mathbf{B}$ - initial analysis for different observation combinations. The dot-dash line represents the true bathymetry $\mathbf{z^t}$. Observations $\mathbf{y}$ are given by circles, the background $\mathbf{z^b}$ by the dashed line and the analysis $\mathbf{z^a}$ by the solid line.

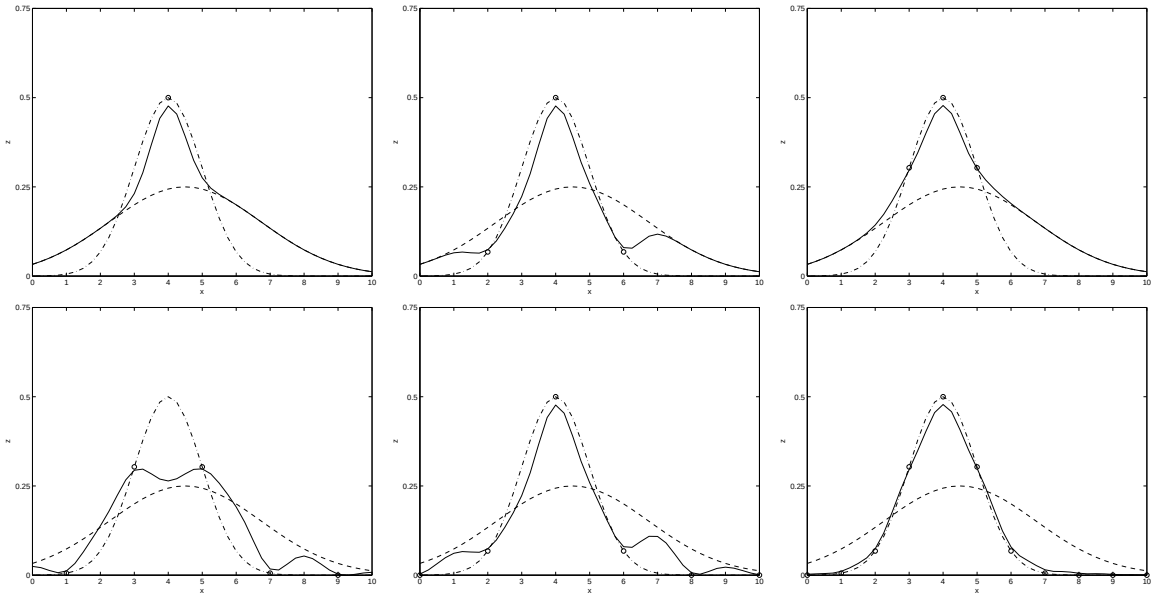

Figure 5.3: Gaussian matrix $\mathbf{B}$ (with $L = 0.5$) - initial analysis for different observation combinations. The dot-dash line represents the true bathymetry $\mathbf{z^t}$. Observations $\mathbf{y}$ are given by circles, the background $\mathbf{z^b}$ by the dashed line and the analysis $\mathbf{z^a}$ by the solid line.

5.2 The Correlation Length Scale

Having concluded that the gaussian matrix $\mathbf{B}$ was most effective in enabling us to produce an analysis that most closely describes the true bathymetry, we now consider the sensitivity of the analysis to changes in the background correlation length scale L.

Recall that the element b_{ij} of the matrix $\mathbf{B}$ defines the background error covariance between the two grid points x_i and x_j. When there is a mismatch between the resolution of the model and the density of the observations these covariances can be used to specify how the observed information is smoothed in model space and therefore control the amount of influence the observations have on the analysis. By varying the size of the background correlation length scale L in (4.5) we can vary the size of the off diagonal matrix $\mathbf{B}$ elements b_{ij}.

The OI algorithm has two effects: it filters noise from the observations and then interpolates the filtered observations to the analysis grid points. Daley (1991) describes a useful technique for investigating the filtering properties of the background error correlations in the OI procedure using an eigenvector decomposition of the background error covariance matrix $\mathbf{B}$. The interested reader is referred to section 4.5 of Daley (1991) for further details. When L is large the covariance (correlation) between the background errors at any pair of grid points is greater. Small scale structures are suppressed, whilst the larger scale structures draw closer to the observations. This generates an analysis that is comparatively smooth. When L is small the background error correlations are reduced. There is less filtering of small scale structures, but the filtering of the large scale structures increases so that away from the observation points the analysis reverts to the background field. Each observation has a much narrower region of effect, and therefore less influence on the analysis.

Figures 5.4 to 5.9 illustrate the effect of different L values for two example observation sets: (i) a single observation at $x = 4$, and (ii) observations at $x = 2$, 4 and 6. The bed is now advected

forward in time with constant celerity $a = 1$ and at each time step a new analysis is produced. Results are given for times $t = 0$ to 3, on the domain $x \in [0, 10]$ with time step $\Delta t = 1$ and grid spacing $\Delta x = 0.1$. As above, we weight in favour of the observations with $\sigma_o^2 = 0.1$ and $\sigma_b^2 = 1$. Again, the dot-dash line represents the true bathymetry $\mathbf{z^t}$, observations $\mathbf{y}$ are given by black circles, the background $\mathbf{z^b}$ by the dashed line and the analysis $\mathbf{z^a}$ by the solid line.

For example (i), the shape of the true solution is captured most accurately with $L = 0.5$ (figure 5.5). If the correlation length scale is halved to $L = 0.25$ (figure 5.4), the peak of the analysis curve is too narrow, oscillations appear at $t = 1$ and proliferate as we continue to move forward in time. With $L = 1$ (figure 5.6) there is too much spreading. The peak of the analysis curve loses height and becomes slightly out of phase with the true bathymetry; although the oscillations have been damped the curve is now too wide. Conversely, the analysis for (ii) improves when we take $L = 1$ (figure 5.8). Initial oscillations produced in the tails of the curve when $L = 0.5$ (figure 5.7) are much smaller and the shape of the analysis is much smoother and closer to that of the true bathymetry. However, if we double the length scale to $L = 2$ (figure 5.9) the radius of influence of each individual observation is too large and the quality of the analysis is noticeably reduced.

We next examine a case where the choice for the L is less distinct. Observation points are positioned at $x = 1$, 3, 5, 7 and 9, so that the peak of the bed is not initially observed. As in the above examples, the true bathymetry moves undistorted with constant celerity $a = 1$. As a way of crudely simulating tidal action, a is reversed at $t = 3$ so that the bed moves back across the domain towards its original starting position. Figures 5.10 and 5.12 compare the analysis produced at each time step for $L = 0.5$ and $L = 1$. The corresponding analysis errors are shown in figures 5.11 and 5.13 respectively.

Although the initial analysis with $L = 0.5$ is poor it soon recovers as the next set of observations are taken and new information becomes available. The analysis errors mirror the movement of the bed and their magnitude is always greatest either side of its peak. Figures 5.11 show that the analysis errors are largest at $t = 0$, from $t = 3$ onwards there are only slight variations in the size and shape of the error plot. At this point the analysis curve lies close to the true bathymetry and continues to do so until final time $t = 7$.

When $L = 1$ the initial profile is oscillation free and although the height of the bed is too low its shape better represents that of the true bathymetry. However, at $t = 1$ this smoothing of the analysis generates errors either side of the observation points that are much larger in magnitude than when $L = 0.5$. As we move through figures 5.12 we see that at times where the peak of the bed is not observed the smoothing of information from the observations either side causes the analysis curve to lose height and creates slight distortion in the tails. At all other times the analysis produced with $L = 1$ is comparable with, or even slightly better than, that produced for $L = 0.5$.

The optimal choice for L appears to depend on a number of factors including the frequency, density and positioning of observations, the type of features and level of detail we wish to resolve, and the quality of the background state. When observations are sparse, a too small L value gives to great an influence to the background state and produces oscillations in the solution. We can create a smoother, more physically realistic analysis by increasing the length scale, but if L becomes too large it can lead to over smoothing, causing loss of detail and the generation of inaccurate values in unobserved regions. When there is a high density of observations, a large L can cause over damping of small scale structures and insufficient filtering of large scale structures leading to an overlap of

information and degradation of the analysis. In order to be able to accurately reconstruct the model state we must ensure that sufficient weight is given to the background state.

6 Conclusions and further work

The aim of this work was to use a simple one-dimensional model of changing bathymetry to illustrate the basic theory of data assimilation and examine some of the issues associated with its practical implementation. We began by introducing the sediment conservation equation and deriving its solution for the special case of constant water height and flux. We then gave a brief overview of data assimilation and presented the OI analysis approach that was used in this work. A simple model based on the linear advection equation was adopted and a series of simple experiments were used to investigate the role of the background error covariance matrix $\mathbf{B}$ in the assimilation process, with results validated against the analytical solution. The correlations in $\mathbf{B}$ govern the spreading and smoothing of the observed information and if they are poorly specified the quality of the analysis can be considerably reduced. We found that for diagonal and tri-diagonal $\mathbf{B}$ matrices there is a lack of information spreading resulting in analyses that oscillate between the observations and background state. A full, symmetric matrix $\mathbf{B}$ constructed using a gaussian function produced much better results. Using a $\mathbf{B}$ matrix of the form (4.5), we were able to increase the radius of influence of the observations allowing the information they contain to be spread further into the model domain. We found that we were able to control the amount of information smoothing using the correlation length scale L and this produced some interesting results.

When there is a mismatch between the spatiotemporal resolution of the model and the density of the observations the correlation length scale L in (4.5) allows us to determine how the observed information is used. Choosing L is a balancing act; we want to extract the maximum amount of information from the observations but we need to limit the amount of smoothing so that the analysis produced is physically accurate. If L is too long the model cannot resolve smaller scale features. However, the importance of being able to do this depends on the nature of the problem we are trying to solve and whether or not these features are an essential part of our analysis. One solution could perhaps be to use a variable length scale that took different values in different parts of the domain.

The correct specification of the background error covariances is a difficult problem and in this report we have only considered three very simple examples. This work could be extended to look at alternative methods for estimating $\mathbf{B}$ such as using innovation (observation minus background) statistics, studying the differences between forecasts that verify at the same time, or from differences in background fields using ensemble techniques [Fisher (2007)].

Throughout these experiments we have assumed that our model is perfect and that we have perfect observations taken from the analytical solution. In reality the model equations do not describe the system behaviour completely, we do not know the true state of the system and all observations we take will contain errors. Adding random noise to the observations would enable us to consider the effect of observation error on the analysis.

The next step is to employ numerical methods. This will allow us to calculate a solution to the sediment conservation equation numerically and investigate the use of data assimilation techniques in the more realistic case (2.3) where $a(z)$ is non-linear.

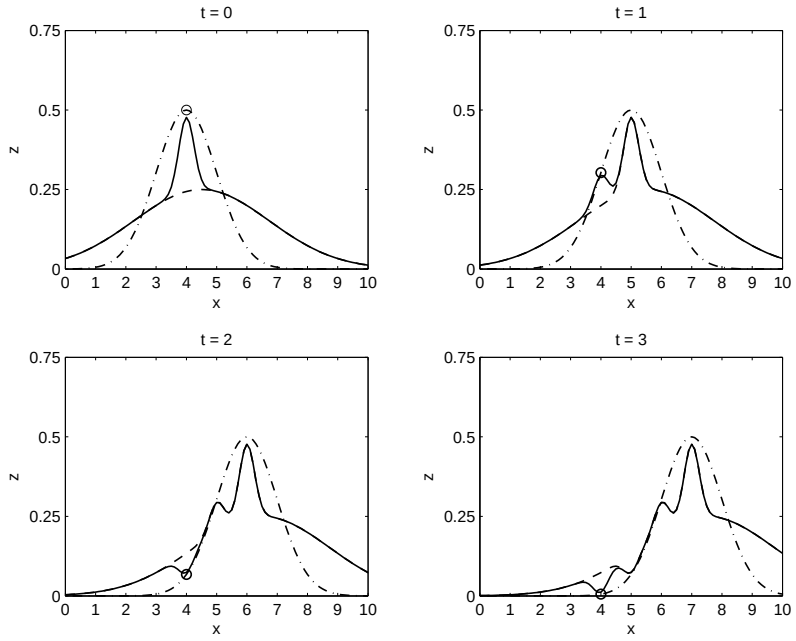

Figure 5.4: Gaussian matrix $\mathbf{B}$ with correlation length scale $L = 0.25$ - analysis with single observation at $x = 4$. The dot-dash line represents the true bathymetry $\mathbf{z^t}$. Observations $\mathbf{y}$ are given by circles, the background $\mathbf{z^b}$ by the dashed line and the analysis $\mathbf{z^a}$ by the solid line.

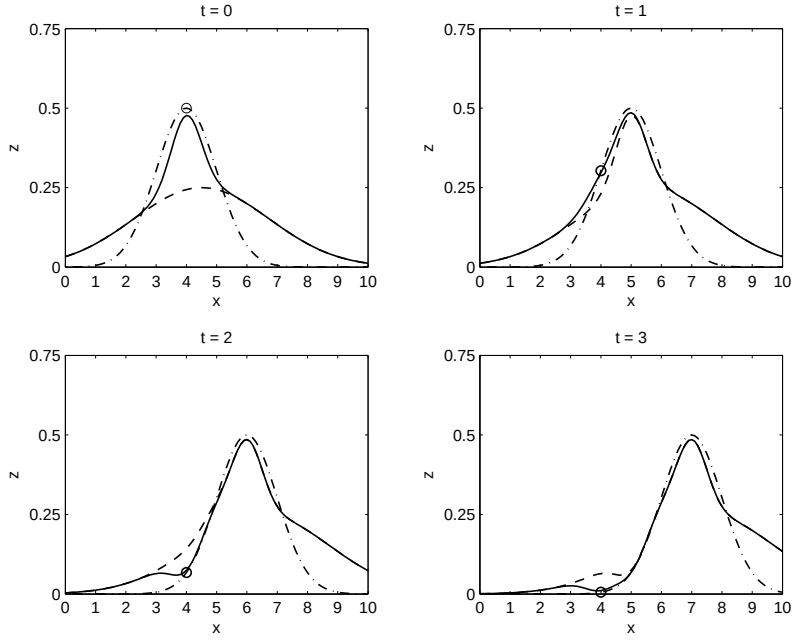

Figure 5.5: Gaussian matrix $\mathbf{B}$ with correlation length scale $L = 0.5$ - analysis with single observation at $x = 4$. The dot-dash line represents the true bathymetry $\mathbf{z^t}$. Observations $\mathbf{y}$ are given by circles, the background $\mathbf{z^b}$ by the dashed line and the analysis $\mathbf{z^a}$ by the solid line.

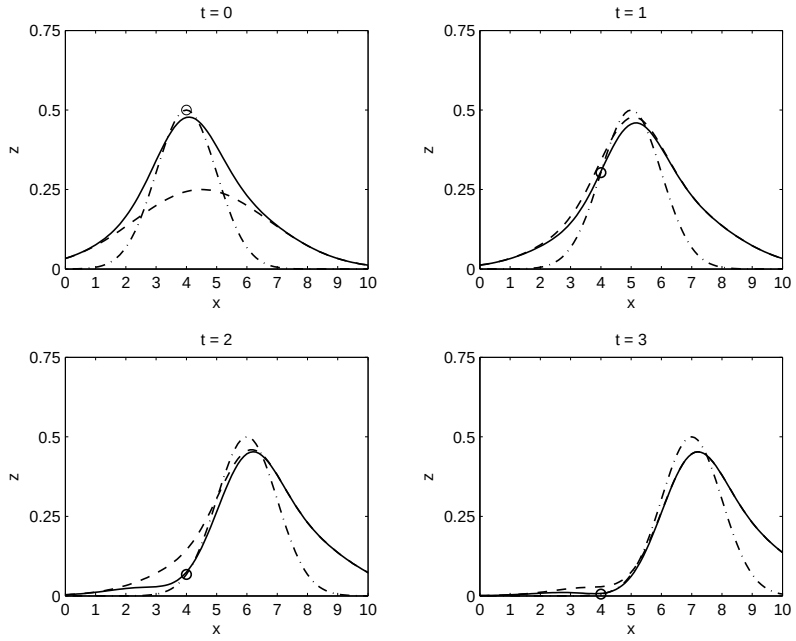

Figure 5.6: Gaussian matrix $\mathbf{B}$ with correlation length scale $L = 1$ - analysis with single observation at $x = 4$. The dot-dash line represents the true bathymetry $\mathbf{z^t}$. Observations $\mathbf{y}$ are given by circles, the background $\mathbf{z^b}$ by the dashed line and the analysis $\mathbf{z^a}$ by the solid line.

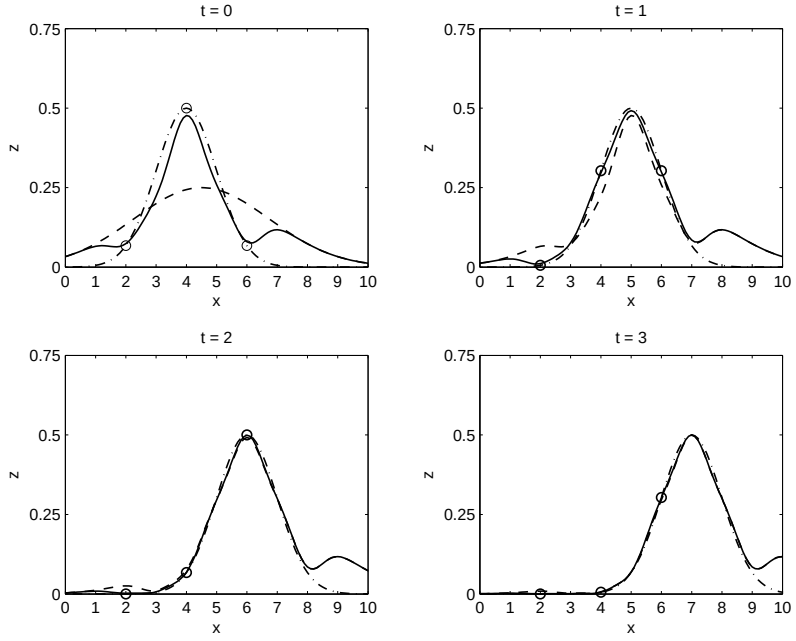

Figure 5.7: Gaussian matrix $\mathbf{B}$ with correlation length scale $L = 0.5$ - analysis with observations at $x = 2$, 4 & 6. The dot-dash line represents the true bathymetry $\mathbf{z^t}$. Observations $\mathbf{y}$ are given by circles, the background $\mathbf{z^b}$ by the dashed line and the analysis $\mathbf{z^a}$ by the solid line.

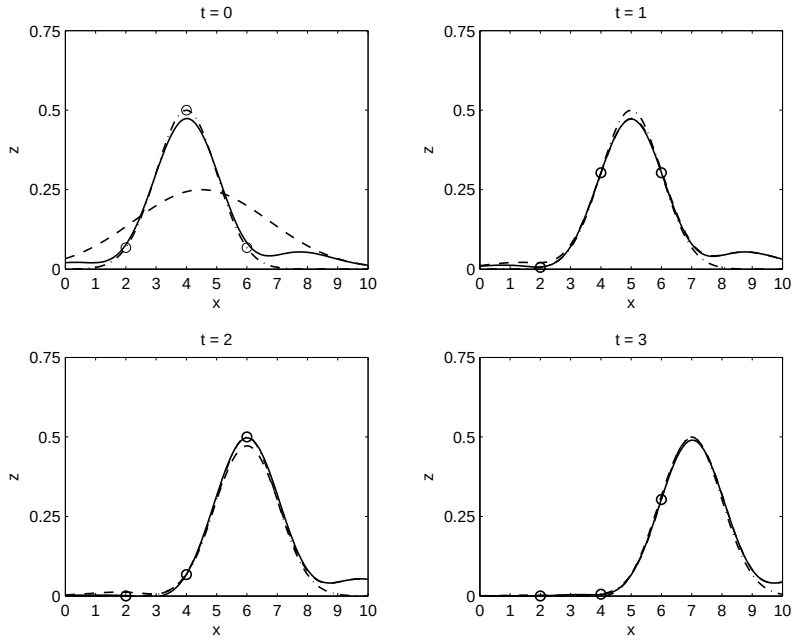

Figure 5.8: Gaussian matrix $\mathbf{B}$ with correlation length scale $L = 1$ - analysis with observations at $x = 2$, 4 & 6. The dot-dash line represents the true bathymetry $\mathbf{z^t}$. Observations $\mathbf{y}$ are given by circles, the background $\mathbf{z^b}$ by the dashed line and the analysis $\mathbf{z^a}$ by the solid line.

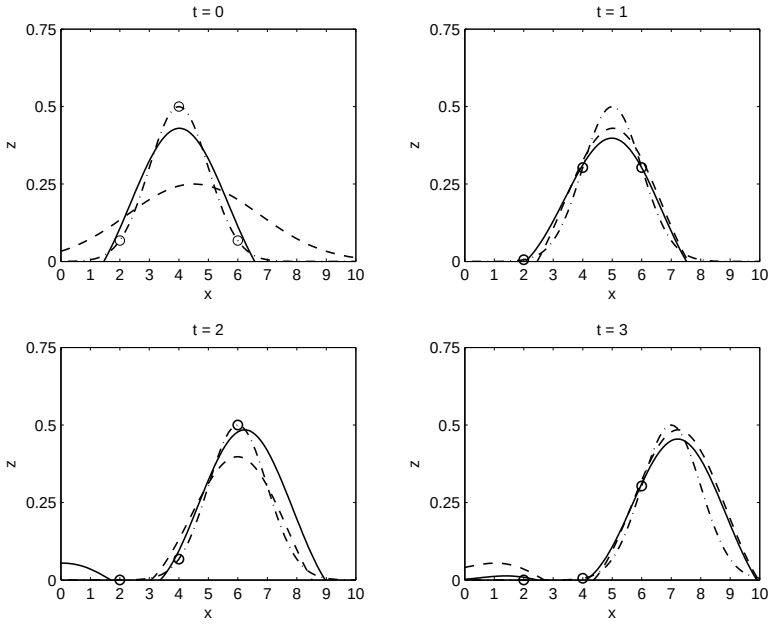

Figure 5.9: Gaussian matrix $\mathbf{B}$ with correlation length scale $L = 2$ - analysis with observations at $x = 2$, 4 & 6. The dot-dash line represents the true bathymetry $\mathbf{z^t}$. Observations $\mathbf{y}$ are given by circles, the background $\mathbf{z^b}$ by the dashed line and the analysis $\mathbf{z^a}$ by the solid line.

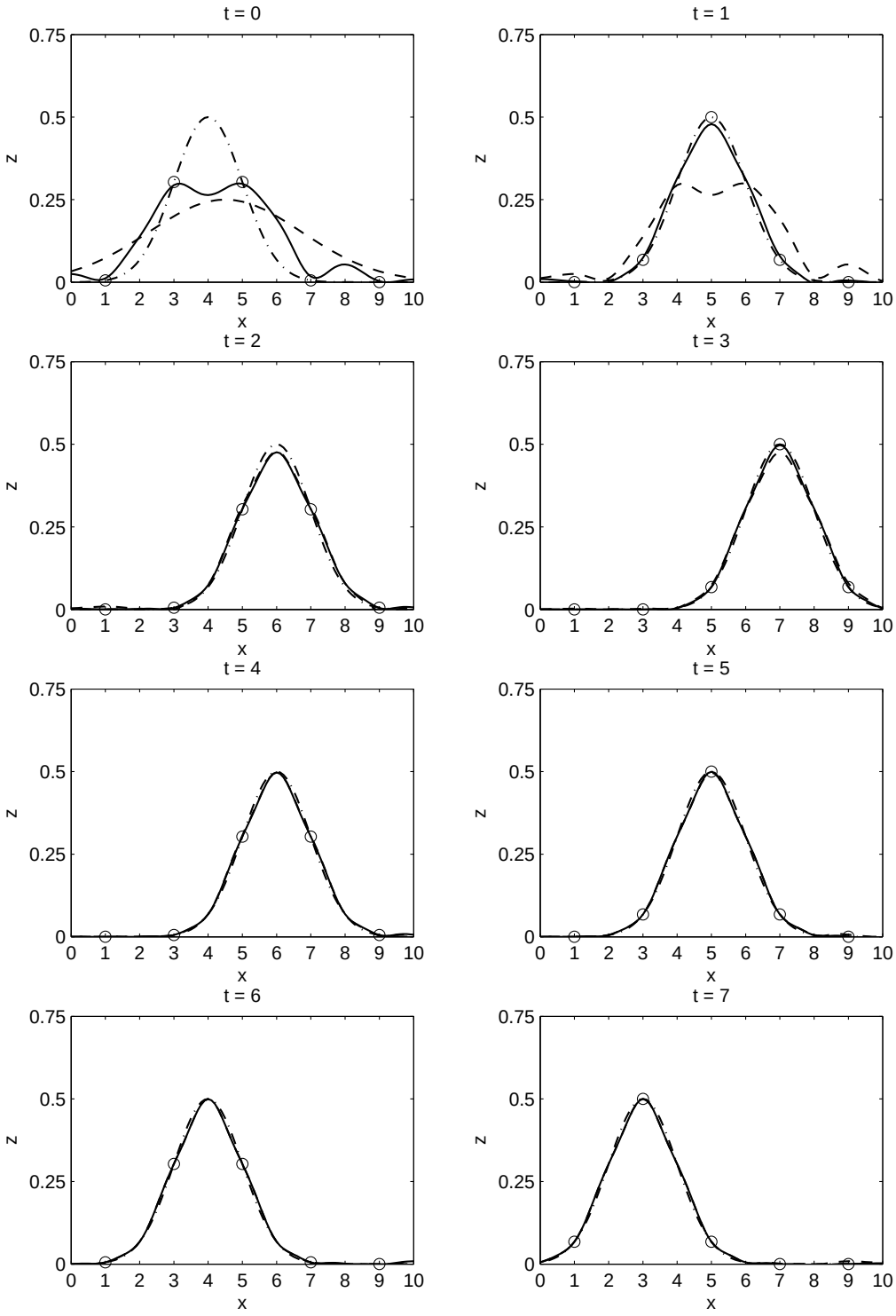

Figure 5.10: Gaussian matrix $\mathbf{B}$ with correlation length scale $L = 0.5$ - analysis with observations at $x = 1$, 3, 5, 7 & 9. The dot-dash line represents the true bathymetry $\mathbf{z^t}$. Observations $\mathbf{y}$ are given by circles, the background $\mathbf{z^b}$ by the dashed line and the analysis $\mathbf{z^a}$ by the solid line.

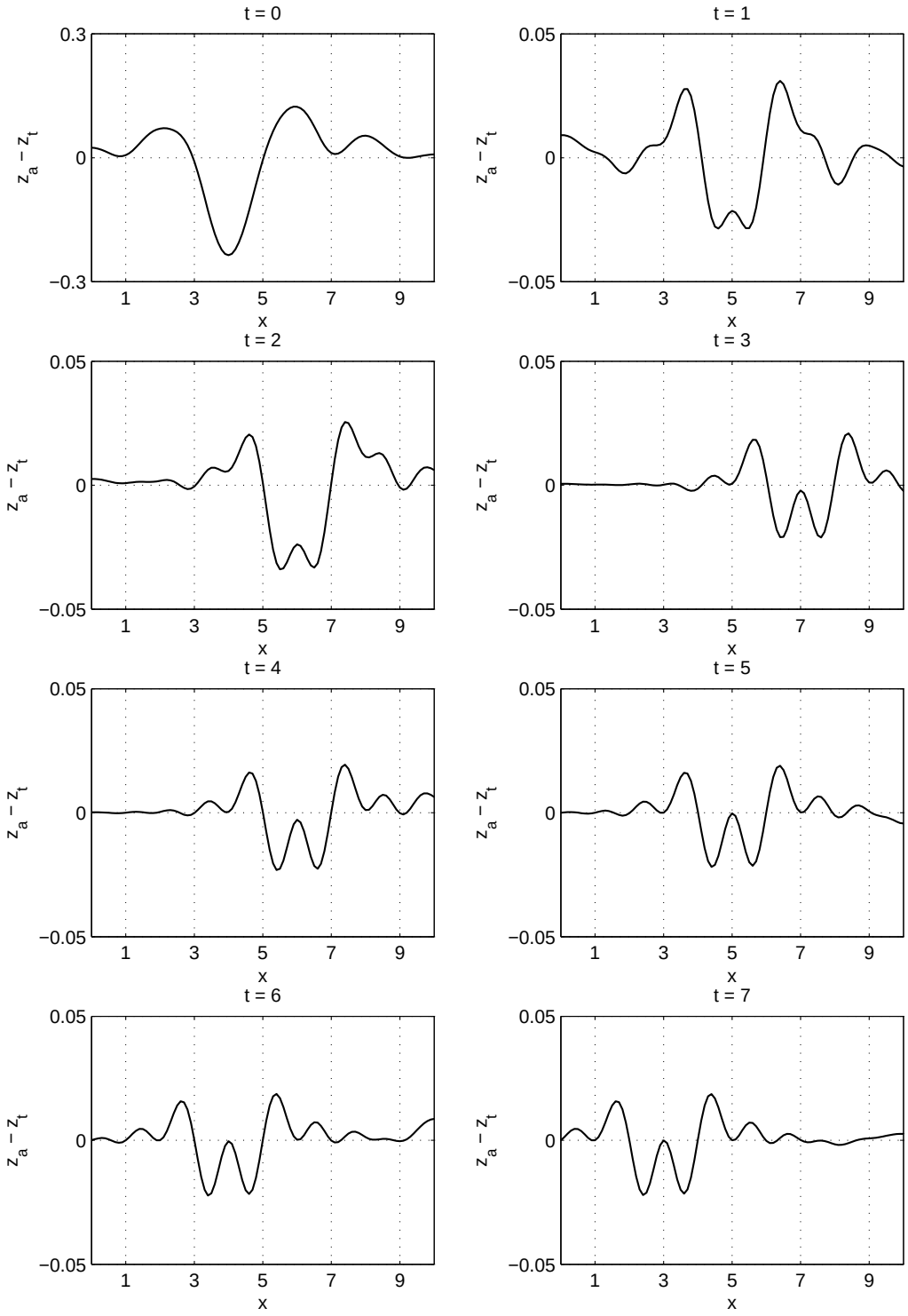

Figure 5.11: Analysis error ($\varepsilon_{\mathbf{a}}$) for gaussian matrix $\mathbf{B}$ with correlation length scale $L = 0.5$ and observations at $x = 1$, 3, 5, 7 & 9 (*note the change in the scale of the errors between times 0 and 1*).

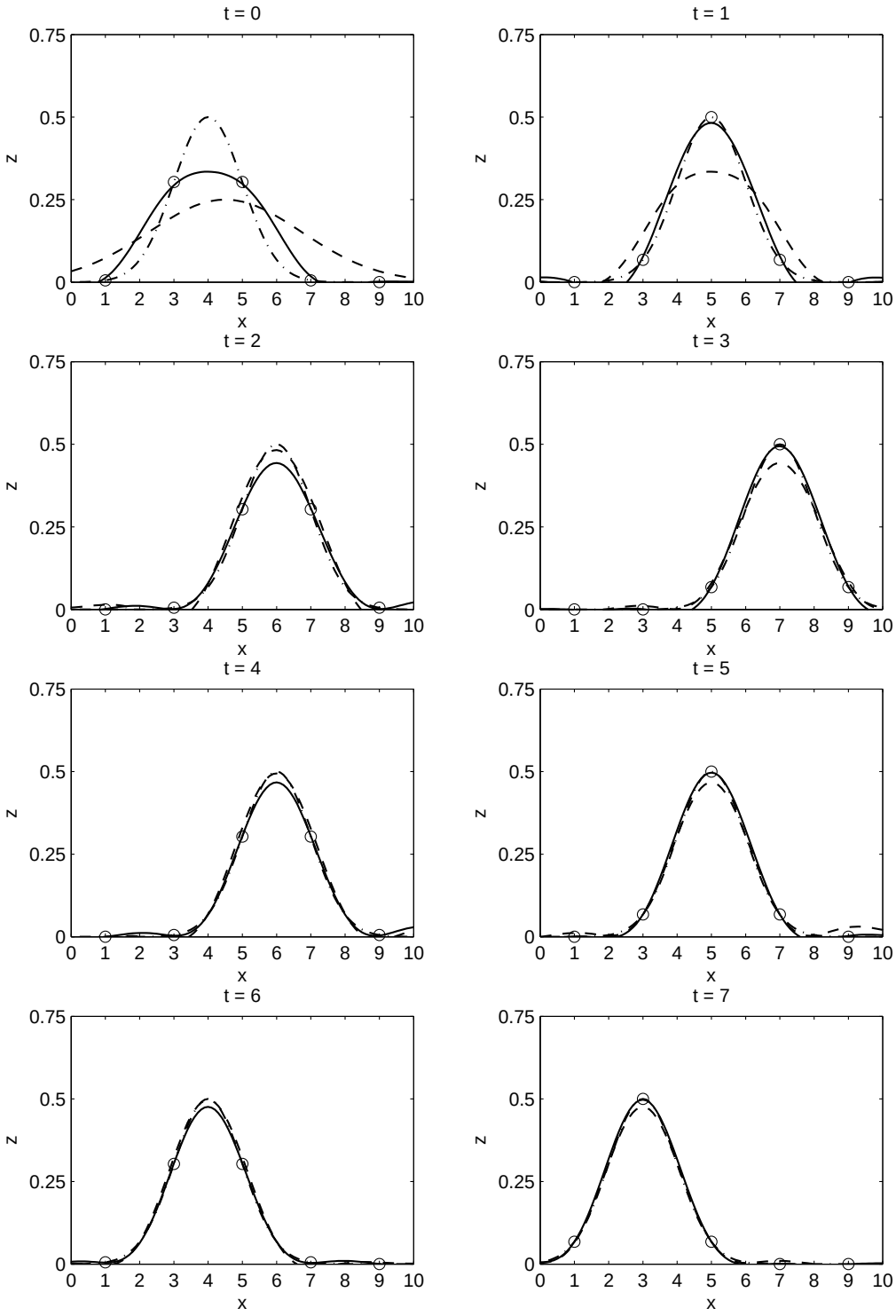

Figure 5.12: Gaussian matrix $\mathbf{B}$ with correlation length scale $L = 1$ - analysis with observations at $x = 1$, 3, 5, 7 & 9. The dot-dash line represents the true bathymetry $\mathbf{z^t}$. Observations $\mathbf{y}$ are given by circles, the background $\mathbf{z^b}$ by the dashed line and the analysis $\mathbf{z^a}$ by the solid line.

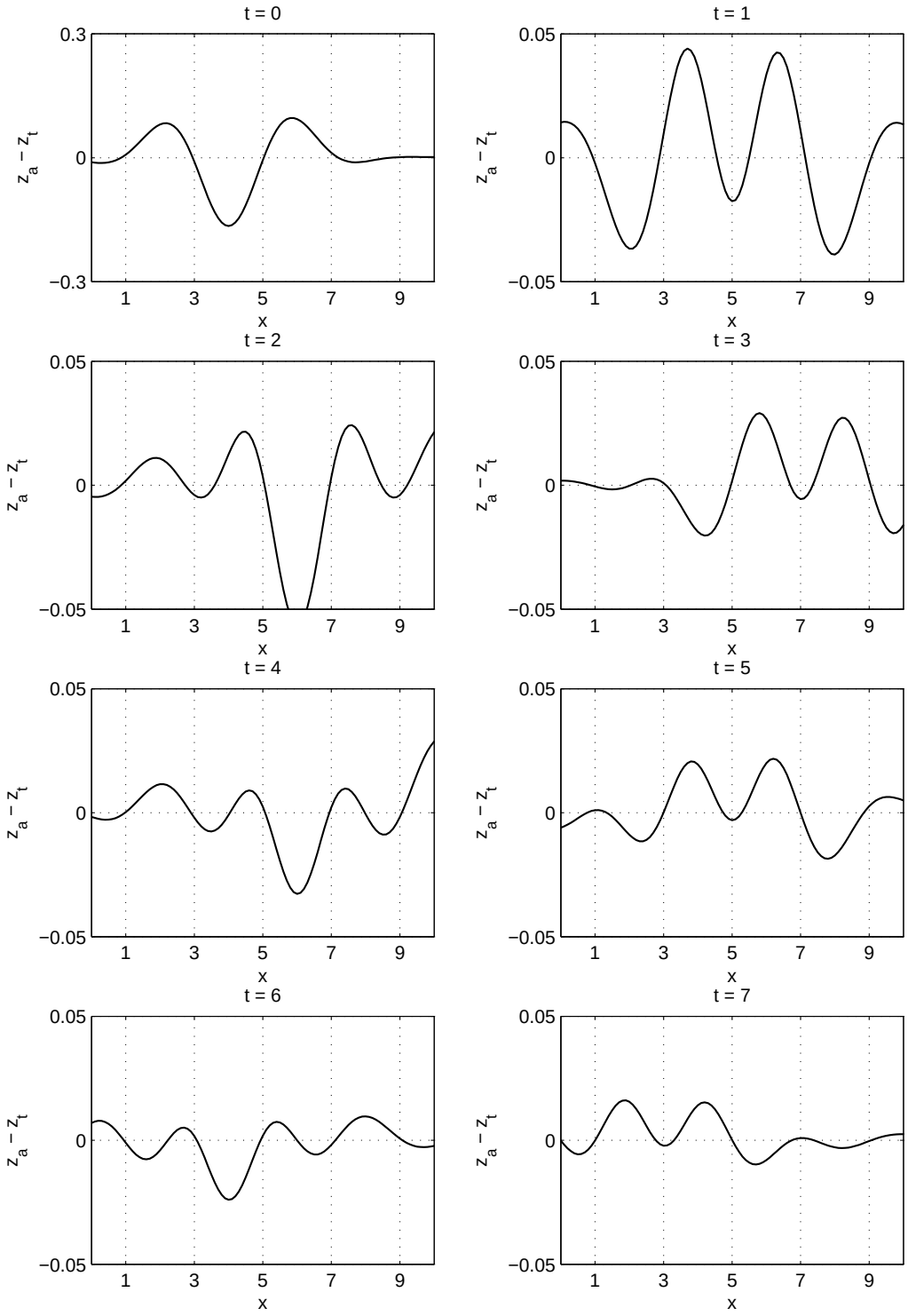

Figure 5.13: Analysis error ($\varepsilon_{\mathbf{a}}$) for gaussian matrix $\mathbf{B}$ with correlation length scale $L = 1$ and observations at $x = 1$, 3, 5, 7 & 9 (*note the change in the scale of the errors between times 0 and 1*).

Acknowledgements

This work is funded under the Natural Environment Research Council (NERC) Flood Risk From Extreme Events (FREE) programme, with additional funding provided by the UK Environment Agency as part of the CASE (Co-operative Awards in Science and Engineering) scheme.

Glossary of Symbols

A	parameter for calculating the sediment transport rate
$a(z, q)$	advection velocity/ bed celerity
F	water flux
h	water height
n	parameter for calculating the sediment transport rate
t	time
$u(x, t)$	depth averaged current
x	horizontal coordinate
z	bathymetry
z_0	initial bathymetry
q	sediment transport rate
ε	sediment porosity
α, β, γ	parameters of the gaussian function
$\mathbf{B}$	background error covariance matrix (dimension $m \times m$)
$\mathbf{h}$	observation operator (from dimension m to p)
$\mathbf{H}$	linearised observation operator (dimension $p \times m$)
$J(\mathbf{z})$	cost function
$\mathbf{K}$	gain matrix (dimension $m \times p$)
m	dimension of the state vector
p	dimension of the observation vector
$\mathbf{R}$	observation error covariance matrix (dimension $p \times p$)
r_{ij}	distance $(x_i - x_j)$ between grid points x_i and x_j
$\mathbf{y}$	vector of observations (dimension p)
$\mathbf{z^t}$	true model state (dimension m)

$\mathbf{z^b}$	background state (dimension m)
$\mathbf{z^a}$	analysis (dimension m)
σ_b^2	background error variance
σ_o^2	observation error variance
$\varepsilon_\mathbf{a}$	vector of analysis errors $z_a - z_t$ (dimension m)
L	background correlation length scale
Δx	spatial resolution

References

Bouttier, F. and Courtier, P. (2002). Data assimilation concepts and methods. Meteorological Training Course Lecture Series. ECMWF.

Daley, R. (1991). *Atmospheric Data Analysis*. Cambridge University Press.

Fisher, M. (2007). Background error covariance modelling. Meteorological Training Course Presentation. ECMWF.

Griffith, A. K. (1997). *Data Assimilation for Numerical Weather Prediction Using Control Theory*. PhD thesis, University of Reading.

Jazwinski, A. H. (1970). *Stochastic Processes and Filtering Theory*. Academic Press.

Kalnay, E. (2003). *Atmospheric Modeling, Data Assimilation and Predictability*. Cambridge University Press.

Lesser, G., Roelvink, J., van Kester, J., and Stelling, G. (2004). Development and validation of a three-dimensional morphological model. *Coastal Engineering*, 51:883–915.

LeVeque, R. J. (1992). *Numerical Methods for Conservation Laws*. Birkhäuser-Verlag.

Lewis, J. M., Lakshmivarahan, S., and Dhall, S. (2006). *Dynamic Data Assimilation: A Least Squares Approach*, volume 104 of *Encyclopedia of Mathematics and its applications*. Cambridge University Press.

Lowe, J. and Gregory, J. (2005). The effect of climate change on storm surges around the united kingdom. *Philosophical Transactions of the Royal Society A*, 363(1831):1313–1328.

Mason, D., Gurney, C., and Kennett, M. (2000). Beach topography mapping - a comparison of techniques. *Journal of Coastal Conservation*, 6:113–124.

Masselink, G. and Hughes, M. G. (2003). *Introduction to Coastal Processes and Geomorphology*. Hodder Arnold.

Nicholls, R., Wong, P., Burkett, V., Codignotto, J., Hay, J., McLean, R., Ragoonaden, S., and Woodroffe, C. (2007). Chapter 6: Coastal systems and low-lying areas. In *Climate Change 2007: Impacts, Adaptation and Vulnerability. Contribution of Working Group II to the Fourth Assessment Report of the Intergovernmental Panel on Climate Change*, pages 315–356. Cambridge University Press.

Nichols, N. K. (2003). Data assimilation: Aims and basic concepts. In Swinbank, R., Shutyaev, V., and Lahoz, W., editors, *Data Assimilation for the Earth System*, volume 26 of *Nato Science Series IV: Earth & Environmental Sciences*, pages 9–20. Kluwer Academic.

Nicholson, J., Broker, I., Roelvink, J., Price, D., Tanguy, J., and Moreno, L. (1997). Intercomparison of coastal area morphodynamic models. *Coastal Engineering*, 31:97–123.

Scott, T. R. and Mason, D. C. (2007). Data assimilation for a coastal area morphodynamic model: Morecambe bay. *Coastal Engineering*, 54:91–109.

Soulsby, R. (1997). *Dynamics of marine sands*. Thomas Telford Publications.

Stelling, G. (2000). A numerical method for inundation simulations. In Yoon, Y., Jun, B., Seoh, B., and Choi, G., editors, *Proc. 4th International Conference on Hydro-Science and Engineering, Seoul, Korea*.

Sutherland, J., Peet, A., and Soulsby, R. (2004). Evaluating the performance of morphological models. *Coastal Engineering*, 51:917–939.

van Rijn, L. C. (1993). *Principles of Sediment Transport in Rivers, Estuaries and Coastal Seas*. Aqua Publications.